# Pozzolanic reactivity of aluminum-rich sewage sludge ash: Influence of calcination process and effect of calcination products on cement hydration

Zhiyang Chang[a], Guangcheng Long[a]*, Youjun Xie [a], John L Zhou[a,b]

[a]School of Civil Engineering, Central South University, 68 Shaoshan South Road, Changsha, Hunan 410075, China

[b]School of Civil and Environmental Engineering, University of Technology Sydney, Sydney, NSW 2007, Australia

*Corresponding author:

Email address: longguangcheng@csu.edu.cn (G. Long)

# Abstract

The application of aluminum-based flocculant in wastewater treatment results in a large amount of Al-rich sewage sludge. This work investigated the influence of calcination process on physicochemical characteristics and pozzolanic activity of Al-rich sludge ash and studied the effect of sludge ash on cement hydration. The results showed that higher calcination temperature from 600 ℃ to 900 ℃ increased the amorphous content in sludge ash. The pozzolanic activity of sludge ash calcined at 800 ℃ and 900 ℃ was confirmed by Frattini test. In view of strength activity index of blended mortar and energy conservation, the optimal calcination process of sewage sludge was calcined at 800 ℃ with air-cooling. The addition of sludge ash accelerated the formation of ettringite and monosulfate phase in cement paste at early hydration age. However, the high Al dissolved concentration of S6 and S7 ash inhibited significantly the cement hydration resulting in low compressive strength of mortar. The pozzolanic reaction of S8 and S9 ash produced more hydration heat and additional Al-bearing products such as katoite and monosulfoaluminate contributing to strength development. Furthermore, the heavy metals in sewage sludge can be immobilized in ash structure after calcination process and the structure of hydration products which ensures the environmental security of sludge ash utilization in construction materials.



*Keywords*: sewage sludge ash; calcination temperature; pozzolanic activity; cement hydration.

# 1 Introduction

Sewage sludge, the byproduct from wastewater treatment, has become a thorny issue for its disposal due to the huge productivity and complicated components [1-2]. With the enhancement of environmental awareness, some traditional disposals of sewage sludge such as ocean dumping have been obsoleted. The decontamination and reclamation of sewage sludge are attracting increasing attention. The agricultural utilization of sewage sludge is limited strictly by the current regulations and modern incineration accounts for more than 50 % of the total sludge disposal, especially for European countries [3-5]. As one of the most environmental-friendly disposals, incineration not only handles cleanly the hazardous and toxic substances in sewage sludge but also reduces $CO_2$ emissions by the cogeneration application. However, a large amount of sewage sludge ash is generated from incineration process. Generally, sludge ash is discarded on waste landfill or used as soil-filling material resulting in a second environmental pollution for soil and groundwater. On the other hand, cement industry produces around 7 % of total $CO_2$ emissions in the world and contributes to 4% of global warming [6]. Thus, there is an urgent demand in exploring alternatives for supplementary cementitious materials to replace cement in the production of low-carbon cement. The recycling of various solid wastes such as fly ash and industrial slag has been a hot area of research for several years [7-8].

Sewage sludge ash consists of high proportion of inorganic oxides such as $SiO_2$, $Al_2O_3$ and CaO, being similar to the chemical composition of pulverized fly ash. Based on this point, extensive studies have explored variety of methods for the potential recycling of sludge ash as a substitution of cement in the production of construction materials, especially in mortars and concretes [9-21]. As reviewed in current studies, the high specific surface area of sludge ash increased water demand of mortar causing a significant loss in workability. Brushite was found in the cement paste blended with sludge ash as a result of the reaction between amorphous iron phosphate with calcium hydroxide [18,22]. The minor elements in ash delayed early cement hydration resulting in a decrease in early compressive strength [19]. However, a reverse effect was

demonstrated by another study where the fine sludge ash particle accelerated cement hydration as it provided more nucleation sites for the precipitation of hydration product [13]. Encouragingly, acceptable mechanical strength and remarkable economic benefit were obtained for that the strength index of mortar with 20% cement substitution by sludge ash decreased merely by 4.5 % as a result of pozzolanic activity [13]. The pozzolanic reaction is a reaction of amorphous phase in supplementary cementitious material with calcium hydroxide to form silicate or aluminate gelatinous products. The pozzolanic activity of sludge ash is highly related to its chemical composition, especially for amorphous and crystalline phases, depending on various factors such as sludge source, treatment additives and calcination process. Generally, finer ash shows a higher pozzolanic activity [20,23]. Recent studies confirm that potential pozzolanic activity of sewage sludge can be activated by thermal treatment whether mono-incineration or co-incineration with other solid wastes [10,24-25].

As reviewed in current literature, sludge ash used in the study was almost obtained from local waste incineration plants indicating that sludge ash was calcined at a certain temperature. As well-known, different calcination treatments will result in a variety of physical and chemical properties of sludge ash. Despites the satisfying results of the sludge ash -blended matrix, there is still more information need to be established about influence of calcination process including calcination temperature and cooling method on the physicochemical characteristics and pozzolanic activity of sewage sludge ash. On the other hand, sludge ash studied in previous research consist of high Ca content (10%~ 40%) which is related to the use of low-cost lime dehydrant in the wastewater treatment [11]. With the development of sewage treatment technology, some inorganic macromolecular compounds such as polymeric aluminum/iron chloride are widely applied in wastewater flocculation process. The application of aluminum-based flocculant in wastewater treatment results in a large amount of Al-rich sewage sludge with low calcium content. The change in chemical composition of sludge ash will make a significant effect on hydration of Portland cement when the ash is used as a supplementary cementitious material. However, little literature has focused on this point so far.

Based on above respect, this paper aimed to study the influence of calcination temperature and cooling technique on physicochemical properties of Al-rich sewage sludge ash. The pozzolanic activity and effect of calcined sludge ash on hydration of Portland cement were also investigated. Firstly, eight samples of sewage sludge were calcined at a temperature from 600 ℃ to 900 ℃ with cooling method of air and water. The physicochemical property of calcined products was characterized by X-ray diffraction, particle size distribution, BET surface area and scanning electron microscopy. Pozzolanic activity of sludge ash was determined in terms of strength activity index of mortar and calcium hydroxide consumption test. Finally, the feasibility of Al-rich sludge ash used as supplementary cementitious material in cement paste were investigated including cement hydration, phase assemblage and pore microstructure of cementitious matrix. The results of this research provided an alternative for recycling of Al-rich sewage sludge by given calcination process.

# 2 Materials and methods

## *2.1 Materials*

Sewage sludge used in this study was collected from West City Sewage Treatment Plant in Changsha. A polymeric aluminum chloride ($AlCl_3$) flocculant is used in wastewater treatment process resulting in a high content of aluminum (17.92 %) and a low calcium content (2 %) in sewage sludge. The sludge was oven dried at 105℃ for 24 h before calcination. P.I 42.5 Portland cement, commercial fly ash and analytical reagent calcium hydroxide were used in this study. A polycarboxylate superplasticizer with a solid content of 40 % was used to adjust the workability of blended slurry. Table 1 presents the chemical compositions and physical properties of raw materials.

**Table 1**

Chemical compositions and physical properties of raw materials

| Oxide | Chemical analysis (% by mass) | | |
|---|---|---|---|
| | Sludge | Cement | Fly ash |

| | | | |
|---|---|---|---|
| $SiO_2$ | 36.43 | 18.07 | 52.70 |
| CaO | 2.00 | 62.86 | 3.70 |
| $Al_2O_3$ | 17.92 | 4.04 | 25.80 |
| $Fe_2O_3$ | 7.61 | 3.41 | 9.70 |
| MgO | 0.98 | 1.68 | 1.20 |
| $Na_2O$ | 0.15 | 0.21 | 0.11 |
| $K_2O$ | 2.41 | 0.661 | 0.03 |
| $P_2O_5$ | 4.60 | 0.24 | -- |
| $SO_3$ | 1.37 | 3.43 | 0.20 |
| $TiO_2$ | 0.76 | 0.32 | -- |
| ZnO | 0.12 | -- | -- |
| CuO | 0.03 | -- | -- |
| MnO | 0.35 | 0.23 | -- |
| LOI | 44.70 | 1.88 | 4.70 |
| Density | 2.8 | 3.2 | 2.2 |

## *2.2 Methods*

### *2.2.1 Sewage sludge calcination*

The dried sewage sludge was calcined at 600 ℃, 700 ℃, 800 ℃ and 900 ℃ for 6 hours in high-temperature resistance furnace. Six-hour of calcination time was used to guarantee sludge fragments being calcined fully and evenly. After calcination, one part of calcined sludge was removed out of furnace in fume hood to be cooled by air and another part was immediately immersed into cold water. The quenching techniques can result in more reactive amorphous phase in ash compared to natural cooling method. The sewage sludge ash calcined at 600 ℃ and cooled by air was named S6-AC while S7-WC means the sample calcined at 700℃ and cooled by water. The water-cooled sludge ash was dried again at 105℃ for 24h. Finally, all samples were milled in crusher for 3min to pass them through a sieve with 150 μm (#100) for later experiment (see Fig.1).

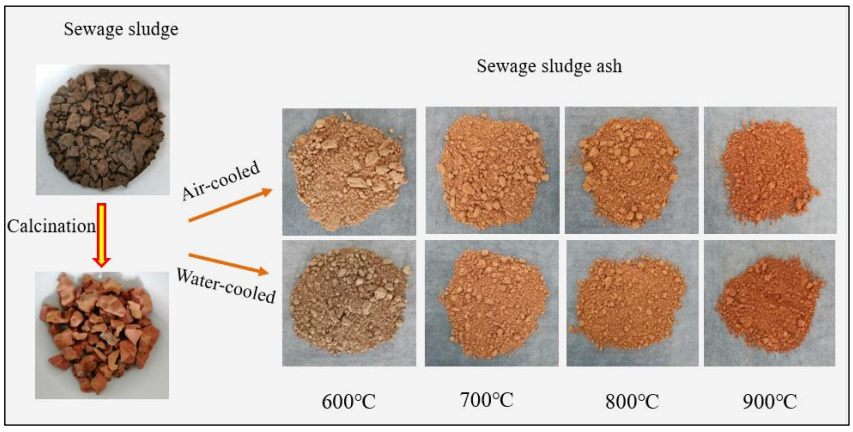


**Fig. 1.** The calcination process of sewage sludge ash.

*2.2.2 Characterization methods*

The chemical composition of sewage sludge ash is obtained by X-ray fluorescence (XRF) using a Bruker S4 Pioneer spectrometer. The mineralogical compositions of ash and blended cement samples are identified by X-ray diffraction (XRD) using a Bruker D8 Advance diffractometer with a 5°-65° (2θ) range and 2°/min rate. The amorphous phase content in ash is quantified by XRD-Rietveld analysis method with 20% ZnO as internal standard material in mixed sample.

Particle size distribution of ash is measured by laser particle scanning analyzer. The specific surface area is determined by BET nitrogen adsorption method. The density is determined by a pycnometer with kerosene as a medium. The water absorption is measured using tea-bag method. Scanning electron microscopy (SEM) is used to observe the morphology of materials with 20.0 kV anode voltage.

*2.2.3 Evaluation of SSA pozzolanic activity*

Three tests, including Frattini test, strength activity index test and calcium hydroxide consumption test are applied to evaluate pozzolanic activity of sludge ash.

*Strength activity index (SAI) test*

The SAI test is an indirect but practical method for evaluating pozzolanic activity of supplementary cementitious material [26-28]. According to ASTM C618-05, a

mortar containing 20% pozzolan and 80% cement requires a minimum of 75% of the 28-day compressive strength of a reference mortar with only cement. In order to present pozzolanic activity obviously in this study, 30 wt% cement was replaced by sludge ash in test mortars (GB/T 1596-2017). The same water/binder ratio (1:2) and sand/binder (3:1) was used for all mortars.

*Frattini test*

Frattini test is conducted by determining the concentration of calcium hydroxide (CH) in aqueous solution containing 30% test pozzolan and 70% cement by weight. The pozzolanic activity of pozzolan is qualified with a lower concentration of calcium hydroxide than the saturation concentration under the same alkalinity. Test samples consisted of 14 g cement, 6 g sludge ash and 100mL boiled deionized water. After mixed fully, the slurries were sealed in a plastic bottle and placed in water bath at 40 ℃ for 8 days. The solution in bottle was then vacuum filtered immediately and cooled to ambient temperature in a sealed bottle. The filtrate was analyzed for [$OH^-$] and [$Ca^{2+}$] by titration with 0.1 M HCl solution and 0.015 M EDTA solution, respectively. The results were plotted with the concentration of [$OH^-$] as the X-axis and [$Ca^{2+}$] as the Y-axis. Solubility curve of calcium hydroxide at 40 ℃ was plotted in the same figure as calibration line. The test point below the calibration line indicated a pozzolanic reaction of sludge ash with calcium hydroxide.

*Calcium hydroxide consumption test*

Calcium hydroxide (CH) consumption test is designed for quantitative analysis of the products and rate of pozzolanic reaction since Frattini test only identifies the pozzolanic activity of sludge ash qualitatively. The mixtures were prepared with a sludge ash: CH : water ratio of 1:1:2 by weight. The samples were placed in water bath at 40 ℃ until test ages. The types and quantity of hydration products were analyzed by XRD-Rietveld method. Calcium hydroxide consumption at different test ages was determined by thermogravimetric analysis.

# 3 Results and discussion

## *3.1 Characterization of sewage sludge ash*

**Table 2**

Chemical and physical property of sewage sludge ash

| Sample | S6-AC | S6-WC | S7-AC | S7-WC | S8-AC | S8-WC | S9-AC | S9-WC |
|---|---|---|---|---|---|---|---|---|
| | Chemical analysis (% by mass) | | | | | | | |
| $SiO_2$ | 44.71 | 44.76 | 45.59 | 45.51 | 45.95 | 46.33 | 46.27 | 46.12 |
| CaO | 2.12 | 2.10 | 2.10 | 2.07 | 2.08 | 2.13 | 2.19 | 2.16 |
| $Al_2O_3$ | 25.55 | 25.5 | 25.71 | 25.83 | 25.52 | 25.61 | 25.01 | 25.12 |
| $Fe_2O_3$ | 8.33 | 8.29 | 8.41 | 8.33 | 8.46 | 8.34 | 8.48 | 8.33 |
| MgO | 1.46 | 1.50 | 1.45 | 1.49 | 1.51 | 1.54 | 1.56 | 1.57 |
| $Na_2O$ | 0.19 | 0.19 | 0.22 | 0.22 | 0.28 | 0.28 | 0.29 | 0.29 |
| $K_2O$ | 2.86 | 2.85 | 2.87 | 2.88 | 2.83 | 2.86 | 2.84 | 2.83 |
| $P_2O_5$ | 5.90 | 5.91 | 5.98 | 6.00 | 5.93 | 5.97 | 5.75 | 5.71 |
| $SO_3$ | 0.92 | 0.88 | 0.71 | 0.81 | 0.42 | 0.45 | 0.12 | 0.12 |
| $TiO_2$ | 0.82 | 0.79 | 0.80 | 0.81 | 0.80 | 0.81 | 0.81 | 0.81 |
| ZnO | 0.13 | 0.13 | 0.13 | 0.13 | 0.14 | 0.13 | 0.13 | 0.13 |
| MnO | 0.36 | 0.36 | 0.36 | 0.37 | 0.35 | 0.36 | 0.35 | 0.35 |
| Amorphous phase | 27.25 | 23.00 | 33.87 | 28.50 | 46.87 | 43.00 | 41.50 | 39.75 |
| LOI (%) | 6.01 | 6.06 | 2.86 | 3.47 | 1.59 | 1.74 | 0.78 | 0.92 |
| | Physical characteristics | | | | | | | |
| Density ($g/cm^3$) | 2.618 | 2.626 | 2.641 | 2.660 | 2.709 | 2.747 | 2.778 | 2.809 |
| $D_{50}$ (μm) | 4.22 | 4.20 | 6.68 | 6.53 | 8.02 | 7.34 | 10.16 | 9.54 |
| BET surface area ($m^2/g$) | 23.286 | 22.123 | 20.558 | 20.516 | 14.516 | 13.910 | 6.849 | 6.805 |
| Water absorption (g/g) | 2.22 | 2.16 | 2.01 | 1.96 | 1.83 | 1.79 | 1.65 | 1.55 |

Table 2 presents the chemical composition and physical property of sewage sludge ash produced from different calcination process. The oxide content of sludge ash was increased within a narrow range due to the decomposition of organics during calcination process. There was a minor variation within 2% in the proportion of oxides such as $SiO_2$, $Al_2O_3$, $Fe_2O_3$ and CaO of sludge ash treated by different calcination process. The content of $Al_2O_3$ in ash was around 25% while the CaO content was only

2%. As compared to cement and fly ash, sludge ash comprised a small number of $P_2O_5$ (about 5%) as a result of organic matter in sewage sludge. It is well-known that pozzolanic activity of supplementary cementitious material is attributed to its siliceous or siliceous-aluminous materials in amorphous phase [6]. As shown in Table 2, the content of amorphous phase in ash increased with calcining temperature from 600 ℃ to 800 ℃ while a decline appeared when the temperature rose to 900 ℃. This value reached a maximum with 46.87 % at 800 ℃ which was regarded as the optimal calcination temperature. Furthermore, the air-cooled ashes had higher content of amorphous material than the ashes cooled by water. It could be explained that a small amount of amorphous phase was dissolved in cooling water which also caused a second water pollution. In the opinion of energy conservation and environmental protection, air cooling was a better alternative than water cooling as well. The physical property of sludge ash such as density and specific surface area was also presented in Table. 2. The density of ash increased from 2.618 to 2.809 g/cm$^3$ with calcination temperature from 600 ℃ to 900 ℃. While a decrease in BET surface area and water absorption was obtained with rising temperature. $D_{50}$ is a median diameter which means that the amount of particle bigger than this size accounts for 50%. As can been seen in Table 2, the $D_{50}$ value of ash increased with increasing temperature.

The SEM images of calcined sludge ash were shown in Fig. 2. As seen in the images, the particle sizes of S8-AC and S8-WC were greater than that of S6-AC and S6-WC. It was also observed obviously that the shapes of sludge ash were irregular with a relatively rough surface. During calcination process, the decomposition of organic matter in sludge resulted in excessive residual pores in ash leading to high BET surface area and water absorption. The sintering and melting of ash occurred with elevated temperature and the open pores of ash particles became closed. Therefore, an increase in density and particle size of ash while a opposite trend in BET surface area and water absorption were obtained. It is worth noting that two cooling techniques had a negligible effect on these physical properties. As can be seen from the results, the physical and chemical properties of ash are highly associated with organic matter pyrolysis, mineral decomposition and crystal transformation during the calcination

process.

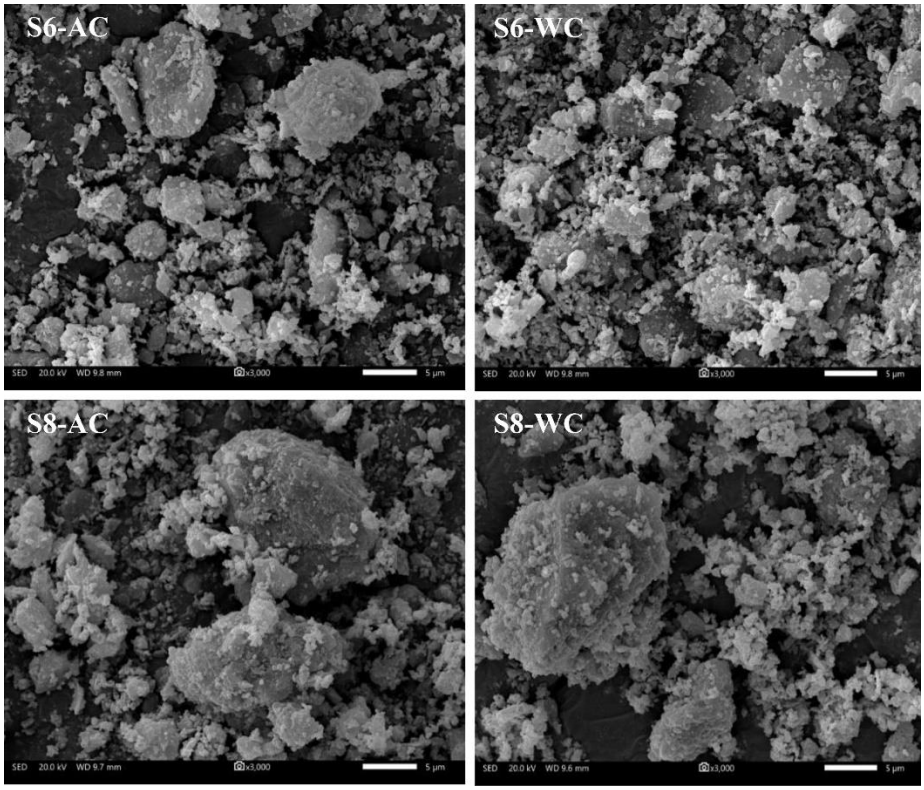


**Fig. 2.** SEM images of sludge ash calcined at 600 ℃ and 800 ℃.

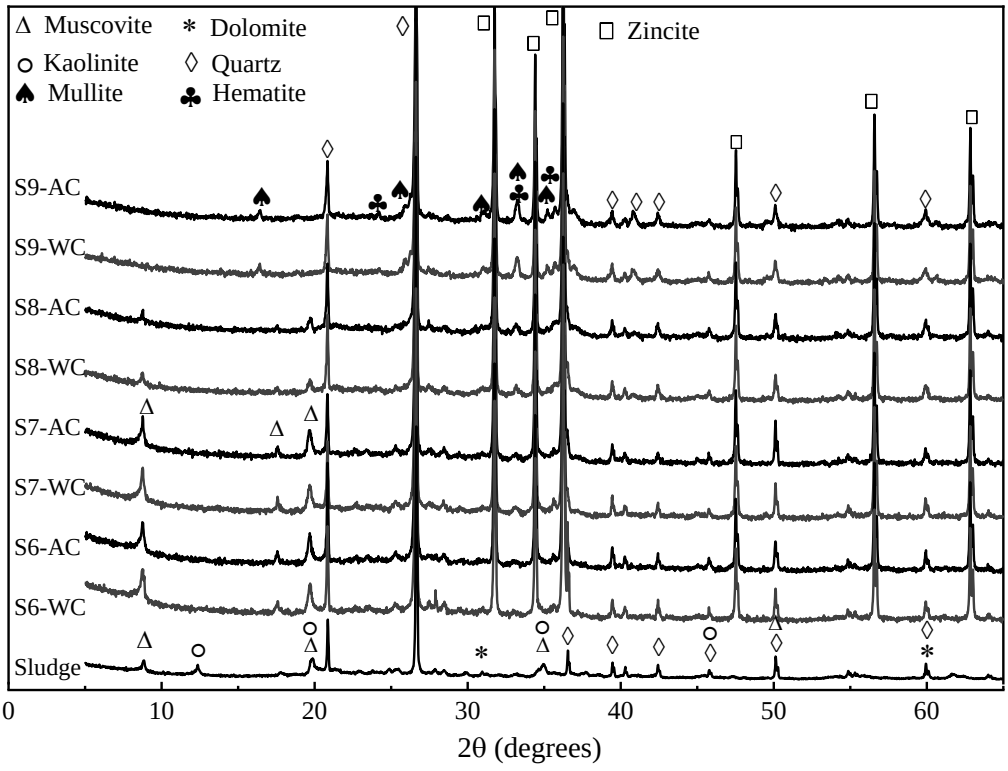


**Fig. 3.** The X-ray diffraction patterns of sewage sludge and calcined ash.

The mineralogical composition of sludge ash was identified by XRD and presented in Fig. 3. Muscovite, quartz, kaolinite and dolomite were main minerals in sewage sludge. During calcination process, kaolinite [$Al_2(Si_2O_5)(OH)_4$] undergoes dehydration and dihydroxylation at the temperature over 500 ℃ [26,29]. Kaolinite is decomposed into reactive $Al_2O_3$ and $SiO_2$ with positive cementitious property [30]. When calcination temperature rises upon 800 ℃, the thermal decomposition of muscovite [$KAl_2(AlSi_3O_{10})(OH)_2$] happens and additional amorphous siliceous or siliceous-aluminous phases are generated in this period [31]. This is the reason why the amorphous phase content of calcined ash increased with calcination temperature. The specific diffractive peak of mullite was found in the XRD patterns of ash calcined at 900 ℃ while muscovite was disappeared due to the exhaustive pyrolysis under this temperature. Mullite is a crystalline-well mineral generated from silicate aluminate under high temperature condition which is an inert component in cementitious materials. Compared with S8-AC, the formation of mullite caused a decline in amorphous phase content of the sample S9-WC and S9-AC. Moreover, the decomposition of dolomite was also observed during calcination process. The transformations of mineral phases in sewage sludge ash during the calcination process are shown as follows:

$$Al_2(Si_2O_5)(OH)_4 \rightarrow Al_2O_3 \cdot 2SiO_2 + 2H_2O \quad (1)$$

$$KAl_2(AlSi_3O_{10})(OH)_2 + SiO_2 \rightarrow KAlSi_3O_8 + Al_2SiO_5 + H_2O \quad (2)$$

$$CaMg(CO_3)_2 \rightarrow CaO + MgO + 2CO_2 \quad (3)$$

In order to investigate the source of reactive matter participating in pozzolanic reaction of sludge ash, the concentrations of main elements in ash such as Al, Si, P, Fe and Mg were determined as sludge ash was dissolved in alkaline solution. The alkaline solution was composed of 0.6 M NaOH and saturated $Ca(OH)_2$ solution for simulating the pore solution of cement paste. The results were shown in Fig. 4. The dissolved concentration was an amount of the element dissolved from 1 g sludge ash. As can been seen in Fig. 4, the dissolved concentration of Fe and Mg was around 0.18~1.20 mg/g which had little effect on aqueous composition of cement paste. The dissolved concentration of Al and P decreased with elevated calcination temperature while the Si concentration was on the contrary. The crystal structure of minerals containing Al and

Si phase can be changed during calcination process. The higher calcination temperature reduced the defective sites of Al phase crystal resulting in a decrease of Al activity [32]. The decomposition of muscovite at high temperature contributed to an increase of Si concentration.

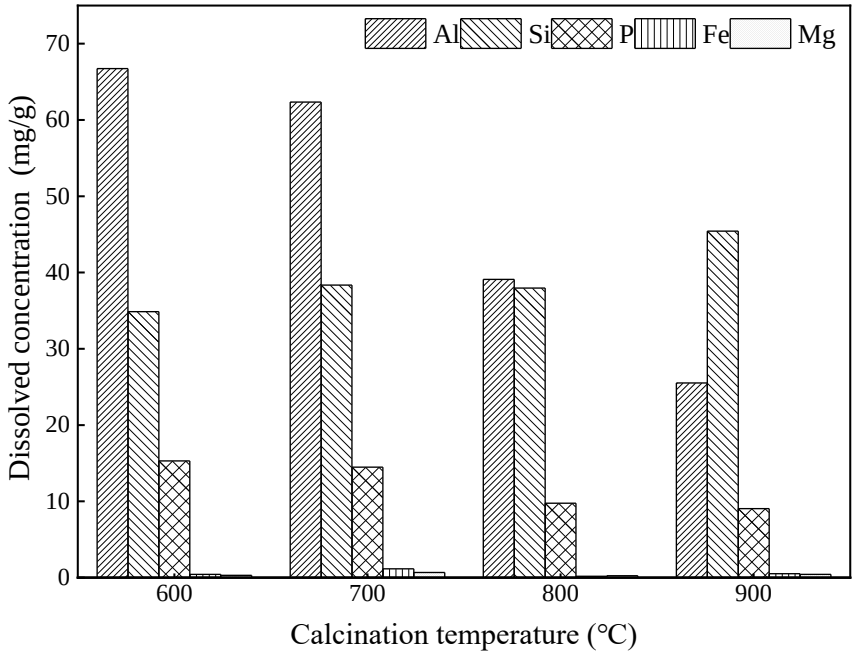


**Fig. 4.** The dissolved concentration of main elements in sludge ash calcined at different temperature.

### *3.2 Pozzolanic activity of sludge ash*

Table 3 Compressive strength (MPa) and strength activity index (%) of sludge ash-modified mortars

| Sample | 3 days | | 28 days | | 90 days | |
|---|---|---|---|---|---|---|
| | CS | SAI | CS | SAI | CS | SAI |
| PC | 24.53 | 100.00 | 39.27 | 100.00 | 47.43 | 100.00 |
| FA | 14.63 | 59.65 | 27.20 | 69.27 | 33.80 | 71.26 |
| S6-AC | -- | -- | 19.87 | 50.59 | 26.60 | 56.08 |
| S6-WC | -- | -- | 19.47 | 49.58 | 25.23 | 53.20 |
| S7-AC | 3.80 | 15.49 | 28.47 | 72.50 | 36.73 | 77.44 |
| S7-WC | 2.70 | 11.01 | 26.70 | 67.99 | 35.77 | 75.42 |

| | | | | | | |
|---|---|---|---|---|---|---|
| S8-AC | 18.33 | 74.72 | 34.57 | 88.03 | 45.10 | 95.05 |
| S8-WC | 19.13 | 77.99 | 32.33 | 82.34 | 43.96 | 92.68 |
| S9-AC | 20.57 | 83.83 | 33.80 | 86.08 | 43.83 | 92.41 |
| S9-WC | 17.90 | 72.96 | 32.03 | 81.58 | 43.57 | 91.86 |

The strength activity index (SAI) test results of mortars containing 30% sludge ash calcined at different temperatures were shown in Table 3. The PC sample with 100% Portland cement was used as control group in the test and FA was prepared with 30% fly ash. At early age, the significant retardation effect of S6 sludge ash on cement hydration led to undetectable compressive strength of mortars at 3 days. The mortars composed of S7 ash also had a low compressive strength. Generally, a material with 75 % of SAI at 28 days is regarded as a standard pozzolan. The 28-day SAI of blended mortars with sludge ash calcined at 800 ℃ and 900 ℃ were over 80 % and the maximum SAI was up to 88.03% for S8-AC sample. The SAI of FA was only 69.27 % which was lower than standard value. Therefore, sludge ash calcined at 800 ℃ and 900 ℃ could be classified as high-activity pozzolan. The SAI increased with the curing age of mortar for all samples and the SAI of S8-AC sample reached a maximum of 95.05 % at age of 90 days. However, a slight reduction in pozzolanic activity of sludge ash calcined at 900 °C was caused by the mineral recrystallization from amorphous to crystalline phase such as mullite. The pozzolanic activity of sludge ash was attributed to amorphous siliceous and aluminous materials transformed by some minerals during calcination process. The high SAI results assure enough mechanical performance of building materials produced with partial substitution of cement by sludge ash.

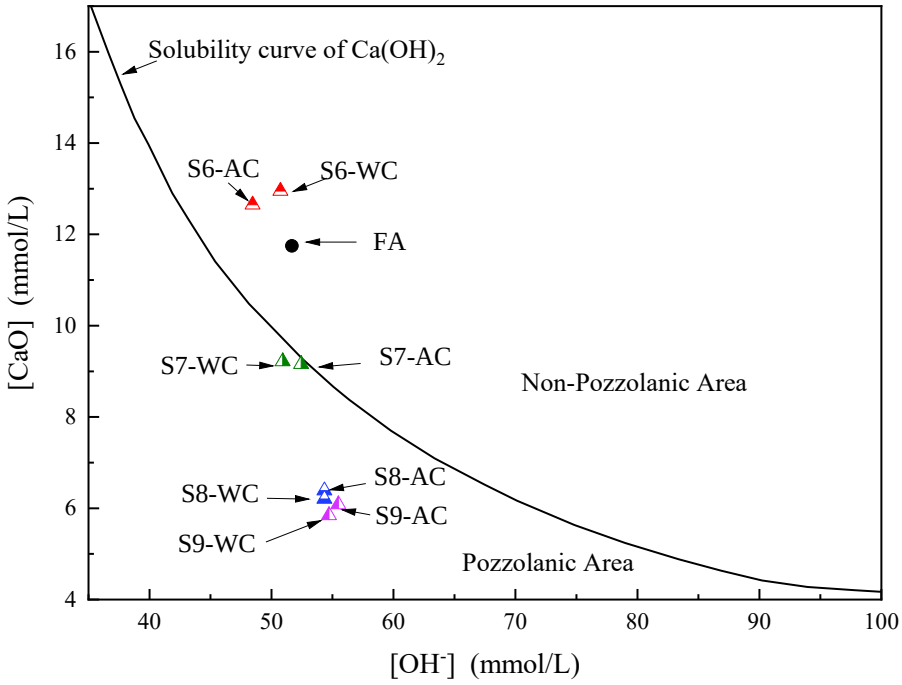


**Fig. 5.** Frattini test results for blended cement containing 30% of sludge ash

Frattini test results for blended paste with 30% cement replaced by different sludge ash were shown in Fig. 5. The test points of S6-AC, S6-WC and FA were located upon the solubility isotherm of $Ca(OH)_2$ where was assumed as no-pozzolanic area. Thus, the sludge ash calcined at 600 ℃ was incompetent for pozzolanic material. For S7-AC and S7-WC, the test results were located near the calibration line which implied the samples had low pozzolanic activity. When the calcination temperature rose up to 800 ℃ and 900 ℃, the location of [CaO] and [$OH^-$] for test samples were far below $Ca(OH)_2$ solubility isotherm, indicating the pozzolanic reaction consumed $Ca^{2+}$ and $OH^-$ released from cement hydration. The sludge ash calcined at 800 ℃ and 900 ℃ could be considered as high active pozzolan which was consistent with the SAI test results.

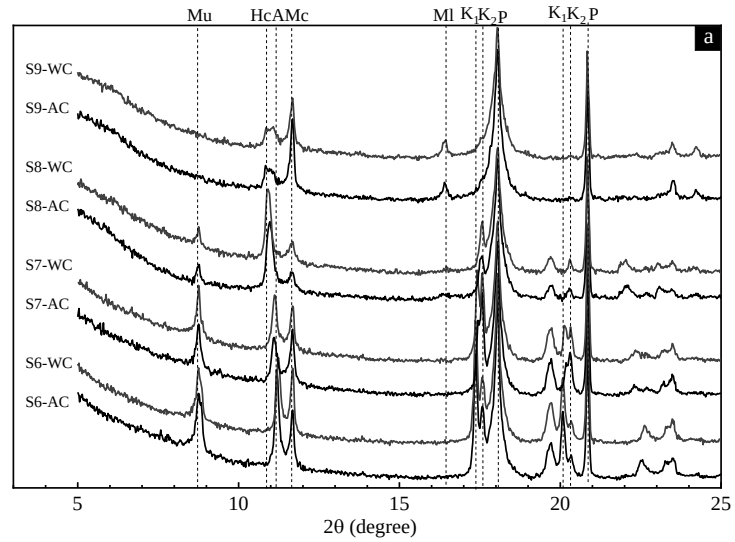


318

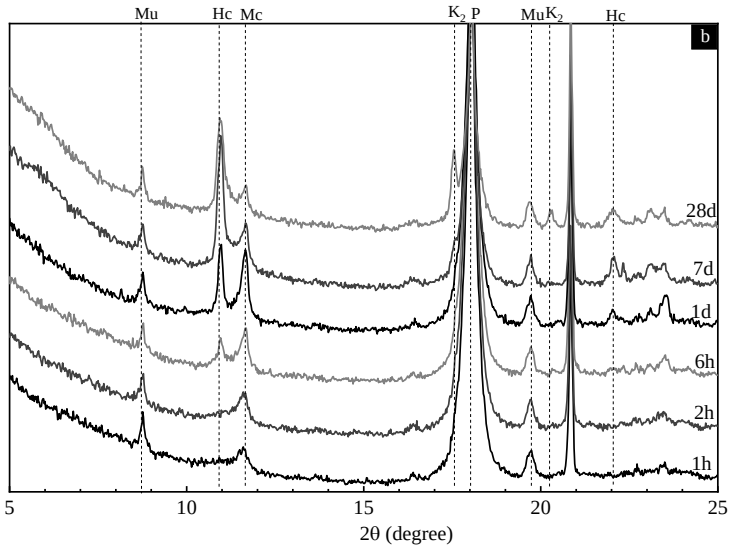


319

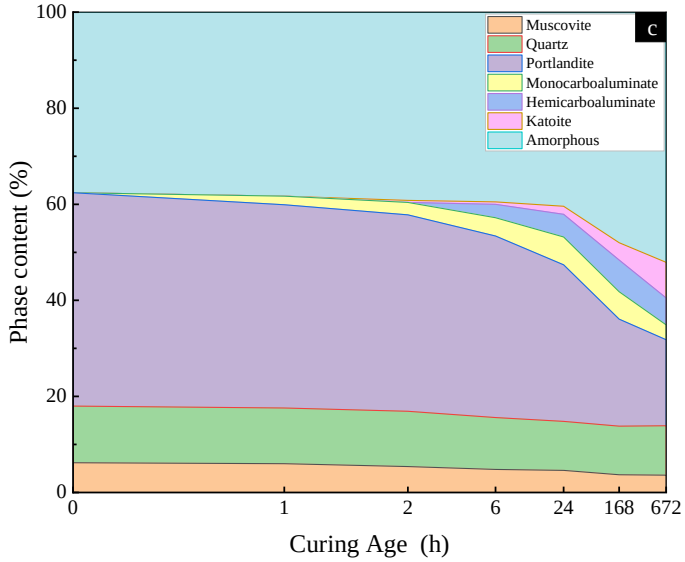


320

321 **Fig. 6.** XRD patterns of mixtures with (a) different sludge ash at age of 28 days, (b) S8 ash at

322 various age and (c) the hydrates evolution with curing age (Mu- muscovite, Hc-

hemicarboaluminate, Mc-monocarboaluminate, A-$H_2AlP_3O_{10}\cdot H_2O$, Ml-mullite, $K_1$-katoite of $Ca_3Al_2(OH)_{12}$, $K_2$-katoite of $Ca_3Al_2(SiO_4)(OH)_8$, P-portlandite).

Calcium hydroxide consumption test was conducted to investigate the phase assemblage in pozzolanic reaction of sludge ash and XRD patterns of hydrates in the sludge ash- CH mixtures were shown in Fig. 6. The XRD patterns presented the characteristic peak of monocarboaluminate [$3CaO\cdot Al_2O_3\cdot CaCO_3\cdot 11H_2O$] for all samples with different sludge ash. The diffraction peak of hydrogen aluminum phosphate hydrate [$H_2AlP_3O_{10}\cdot H_2O$] was also observed for the mixtures with sludge ash calcined at 600 ℃ and 700 ℃. The formation of $H_2AlP_3O_{10}\cdot H_2O$ was a result of the reaction of aluminum ion with the soluble phosphates in sludge ash. The dissolved Al from S6 and S7 ash reacted with portlandite to form katoite [$Ca_3Al_2(OH)_{12}$]. For the samples with S8-AC/WC, the content of hemicarboaluminate [$4CaO\cdot Al_2O_3\cdot (CO_3)_{0.5}\cdot 12H_2O$] increased with a decrease in monocarboaluminate content. The Si-bearing katoite [$Ca_3Al_2(SiO_4)(OH)_8$] was also generated with the participation of [$SiO_4$] introduced from sludge ash. The mount of katoite was declined with calcination temperature attributing to the decrease of Al dissolved degree in sludge ash. The diffraction peak of katoite disappeared in the mixtures with S9-AC/WC. The phase evolution of hydration products in the mixture with curing age was shown in Fig. 6 (b). Monocarboaluminate was found at the initial age and it content increased with hydration time. At age of 1 d, the transformation of monocarboaluminate into hemicarboaluminate was identified with a decrease of monocarboaluminate content. Furthermore, the hydration products like C-S-H gel are usually identified as amorphous phase. The amount of hydration phase was quantified using XRD-Rietveld refinement and TG analysis, as given in Fig. 6 (c). The content of quartz and muscovite varied slightly with curing age due to the inert nature. The reactive aluminium and silicon phase of sludge ash was dissolved in solution and reacted with portlandite. Katoite was produced from a reaction of $Ca^{2+}$ with [Al $(OH)_4]^-$ and $[SiO_4]^{4-}$ in the solution. At age of 28 day, the content of katoite was determined around 7.4 %. Furthermore, the amount of amorphous phase increased with curing age from 37.6 % at initial time to 52.1 % at 28 days. In contrast, the content of portlandite was consumed by 24.4 %. It should be

noted that the rate of portlandite consumption was fast with 0.4 % per hour during the first 24 hour while the portlandite consumption was measured only 10.3 % and 4.4 % in the next 6 days and 21days, respectively. Thus, it can be seen the pozzolanic reaction of sludge ash was carried out at early hydration age and contributed to a strength activity index over 80 % at seven days.

### *3.3 Effect of SSA on cement hydration*

#### *3.3.1 Hydration heat evolution*

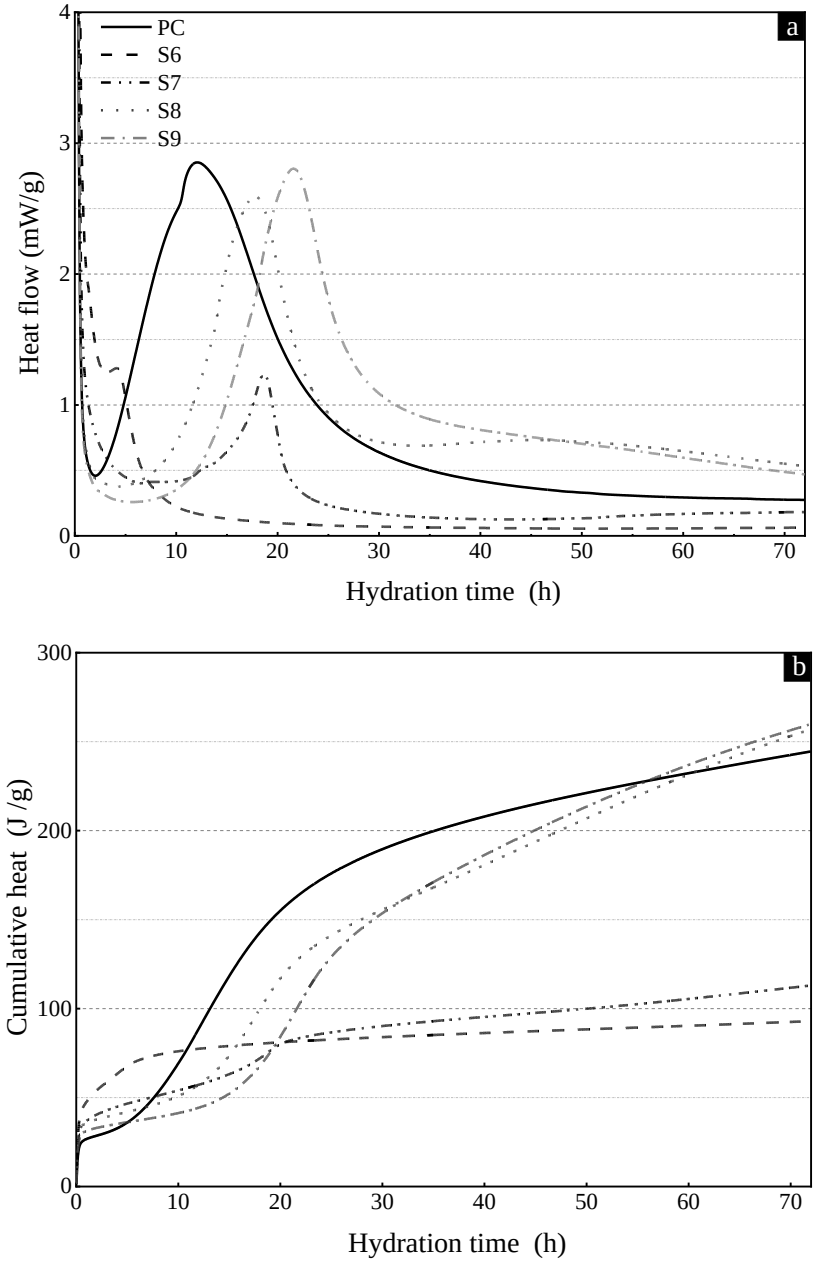


**Fig. 7.** The (a) hydration heat flow and (b) cumulative heat of cement pastes (normalized to the amount of cement).

The hydration exothermic evolution of cement pastes blend with 20 % sludge ash were measured by isothermal calorimetry and the hydration heat rate and cumulative heat of mixtures were illustrated in Fig. 7. A significant difference was found in the curves of pastes with the addition of different sludge ash. For the pastes with S8 and S9 ash, the results showed a similar change of hydration heat to the reference PC (100% cement). The peak value of two pastes was 2.60 mW/g and 2.81 mW/g which was comparable to that of PC paste (2.85 mW/g). As can be seen in Fig. 7 (a), the induction period was delayed by sludge ash of S8 and S9 about 6~8 hours corresponding to a retardation of alite ($C_3S$) hydration. Interestingly, a second mild exothermic peak occurred at 40 h~ 60 h in the S8 paste which was attributed to the pozzolanic reaction of sludge ash. However, the addition of S6 and S7 ash had a significant inhibition effect on cement hydration. For the S6 paste, the first exothermic peak emerged early at 4 h of hydration with a peak value of 1.28mW/g. After 10 hours, a very low heat release rate was maintained until the end of hydration heat test. The first peak of the S7 paste appeared at around 18.7 h of hydration and then the heat release rate decreased quickly in the next 2 hours. As shown in Fig. 7 (b), the initial hydration heat was increased with the addition of sludge ash. In the first 10 hour, the S6 paste presented the highest hydration heat, but it was increased stagnantly later for a long time. After 60 h of hydration, the cumulative hydration heat of S8 and S9 paste exceeded that of PC paste as an existence of pozzolanic reaction.

The retarding effect of sludge ash can be explained by the dissolution of reactive aluminum and phosphorus in ash. The content of soluble Al and P was highest in S6 ash (see Fig. 4). The addition of Al dissolved from sludge ash promoted the reaction of aluminate and sulfate to produce ettringite and Al-bearing hydration products. Aluminum ions were covalently bound to the surface of $C_3S$ in the form of aluminosilicate products rather than physical adsorption [33]. Thus, the formation of additional hydrates increased the initial hydration heat of cement and inhibited the hydration reaction of $C_3S$. The similar retard effect is observed in the study of Al-rich supplementary cementitious materials [34]. Furthermore, the existence of phosphate

anions dissolved from ash also delay the cement hydration [35-36]. Even though the induction period of cement hydration was delayed by S8 and S9 ash, the subsequent pozzolanic reaction of amorphous phases in ash with portlandite contributed to more hydration heat compared with the reference.

*3.3.2 Hydration phases assemblage*

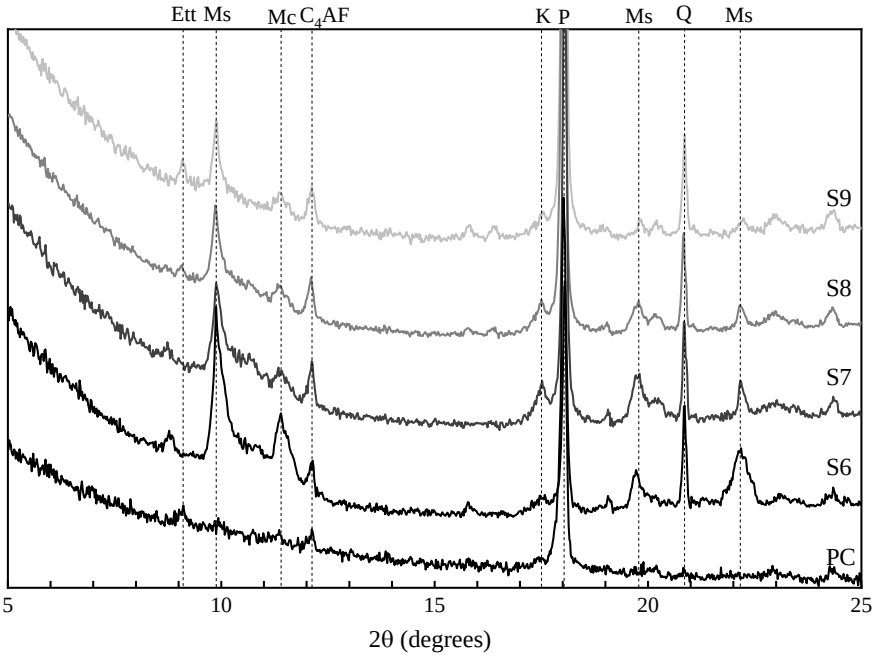


**Fig. 8.** XRD patterns of cement paste blended with sludge ash curing at 28 days (Ett- ettringite, Ms- monosulfoaluminate, Mc-monocarboaluminate, K-katoite, P-portlandite, Q-quartz)

Fig. 8 showed the XRD patterns of cement pastes blended with sludge ash at the curing age of 28 days. The diffraction peak of ettringite was discerned in the XRD pattern of PC, S8 and S9 paste. As compared with PC paste, the monosulfoaluminate and katoite phase were observed in the pastes with sludge ash and the S6 paste owned the highest peak value of monosulfoaluminate. In the cement paste, ettringite was generated from the reaction of Ca, Al and $SO_4^{2-}$ and the transformation of ettringite into monosulfoaluminate occurred as gypsum was depleted. For the S6 and S7 paste, the additional Al from sludge ash accelerated the consumption of gypsum and promoted the transformation of monosulfoaluminate. Thus, the ettringite was not identified in these two pastes. In addition, monocarboaluminate was converted from ettringite as

carbonate-bearing monosulfate phase resulting from the presentence of aluminum [37]. However, phosphate hydrates such as brushite, whitlockite or hydroxyapatite were not presented in this study due to low content of phosphate in sludge ash.

*3.3.3 Microstructure of blended paste*

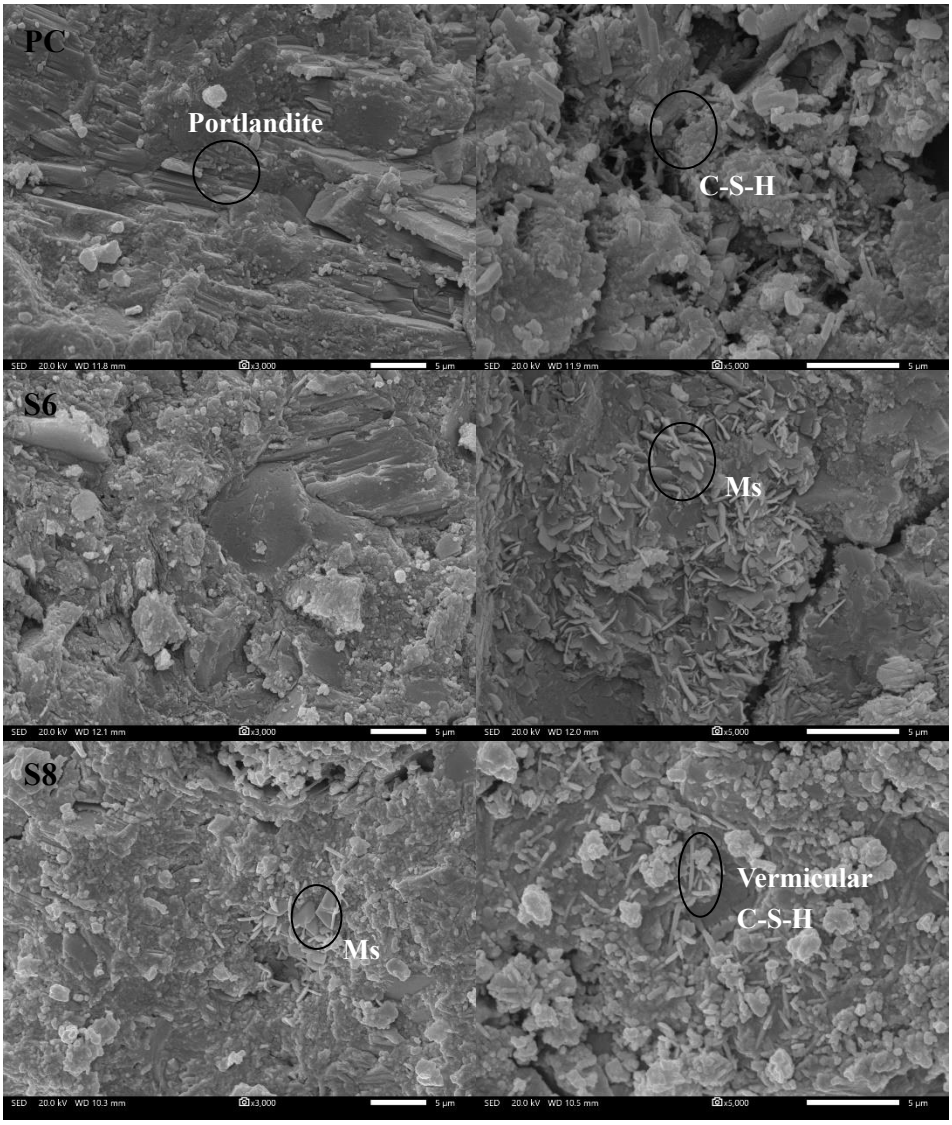


**Fig. 9.** SEM micrographs of cement pastes blended with sludge ash.

The SEM images of cement pastes with 20% sludge ash were presented in Fig. 9. In PC paste, portlandite with good crystallinity were layered together to form a dense structure and the C-S-H gel formed from cement hydration was interspersed with the needle-shaped ettringite. With the addition of sludge ash, more discernible pores were observed in cement pastes resulting in a loose microstructure. These pores not filled by

hydration products would have an adverse effect on the mechanical performance of cement paste. The monocarboaluminate phase with hexagonal sheet-shaped crystal were identified in the S6 and S8 paste. The SEM images of S8 paste showed the formation of short rod-like and vermicular C-S-H gel since the introduce of additional Si and Al from sludge ash decreased the Ca/Si ratio of gel. However, the C-S-H gel with diverse morphology cannot be discerned as the hydrate of cement hydration or pozzolanic reaction of sludge ash. The effect of sludge ash on the calcium silicate hydrate gel including element composition and morphology need to be further investigated.

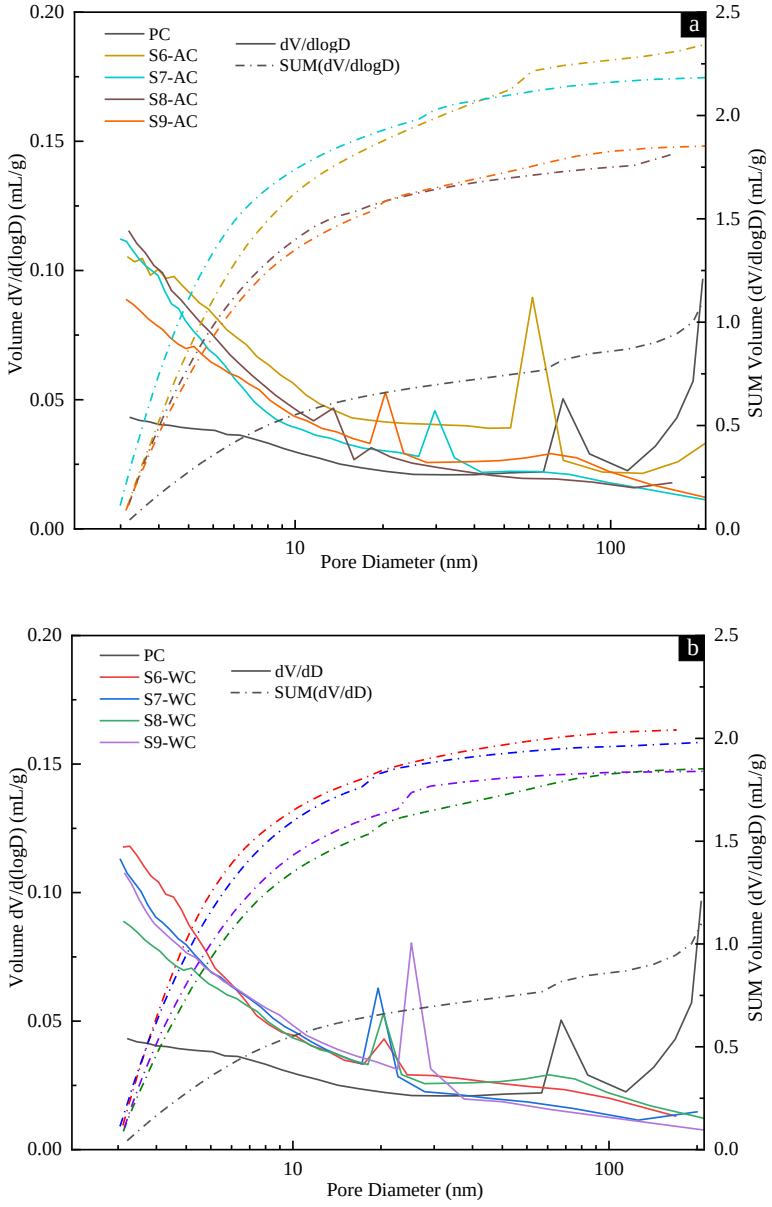


**Fig. 10.** Pore size distributions of cement pastes measured by BET method.

The pores structures of cement pastes were determined by the BET nitrogen adsorption method [38-39] and the test results were showed in Fig. 10. An increase in the pore volume was recognized in cement pastes with the incorporation of different sludge ash. It can be explained by the porous characteristics of sludge ash which was derived from the decomposition of organic matter in sludge during calcination process. Furthermore, the variety in type and structure of hydration products at the presence of ash resulted in more pores in paste structure as can be seen in SEM images as well. It is worth mentioning that the amount of pore over 50 nm in the blended pastes was reduced gradually in comparison to the control. This test result could indicate that the large pores of cement paste might be partially or totally filled by the addition hydration products from pozzolanic reaction of sludge ash. The test results of pores structure are consistent with the SAI results and further confirm the occurrence of sludge ash pozzolanic activity which is beneficial to strength development.

### *3.4 Leaching behavior of mortars with sludge ash*

**Table 4**

Leaching concentrations of mortars using the TCLP.

| Sample | Concentration of heavy metals (mg/L) | | | | | | |
|---|---|---|---|---|---|---|---|
| | As | Cd | Cr | Cu | Ni | Pb | Zn |
| Sludge | 0.03 | 0.02 | 0.02 | 0.22 | 0.55 | 0.01 | 7.30 |
| S6 | 0.56 | 0.006 | 0.14 | 0.24 | 0.20 | 0.07 | 4.30 |
| S7 | 0.46 | 0.005 | 0.05 | 0.25 | 0.11 | 0.04 | 3.00 |
| S8 | 0.38 | 0.002 | 0.01 | 0.16 | 0.04 | 0.02 | 0.31 |
| S9 | 0.42 | 0.003 | 0.02 | 0.18 | 0.047 | 0.02 | 0.19 |
| M6 | 0.001 | ND | 0.38 | 0.006 | 0.002 | ND | 0.004 |
| M7 | 0.003 | ND | 0.37 | 0.005 | 0.005 | 0.004 | 0.004 |
| M8 | 0.004 | ND | 0.33 | 0.001 | 0.004 | ND | 0.001 |
| M9 | 0.003 | ND | 0.35 | ND | ND | ND | ND |
| FA | 0.002 | ND | 0.11 | 0.002 | ND | ND | ND |

| | | | | | | | |
|---|---|---|---|---|---|---|---|
| PC | ND | ND | 0.32 | 0.003 | ND | 0.005 | 0.001 |
| TCLP Regulatory Limit | 5 | 1 | 5 | 15 | 25 | 5 | 25 |

ND: not detected; S6~S9-sludge ash; M6~M9-mortar blended with 30% sludge ash.

Heavy metal pollutants such as Cr and Pb in sewage sludge is a significant concern when it is used in construction materials [40-42]. In order to ensure the security of sludge ash utilization, toxic characteristic leaching procedure (TCLP) was adopted to determine the leaching concentrations of raw sewage sludge, sludge ash and mortars blended with sludge ash. The TCLP test result as shown in Table 4 indicated that the leaching concentrations of heavy metals for all samples were far below the regulatory limit. In sewage sludge, the concentration of Zn was higher than other minor components. The direct utilization of sewage sludge may introduce contaminants to the finished products and cause the secondary environmental pollution. After the pretreatment of the incineration process, most of organic matter in raw sludge was decomposed and the leaching concentrations of heavy metals was declined with the elevated calcination temperature. The glassy and crystalline products generated from the sintering process could incorporate metal ions into the amorphous network and crystal structure resulting in the immobilization of heavy metals [43-44]. The mortars with 30 % sludge ash showed lower leaching levels compared to sludge ash except for Cr element which might come from the cement. In cement paste, the heavy metals could be embedded into the structure of hydration products or react with other ions to form precipitates [45]. Furthermore, the dense structure of cement paste prevents the leaching behavior of heavy metals. In conclusion, the immobilization of heavy metals in calcination process and cement paste guarantee the security about the future utilization of sludge ash in construction materials.

# 4 Conclusion

Based on the test results and analysis in this study, the conclusions are drawn as follows:

(1) The main oxides of Al-rich sludge ash were $SiO_2$, $Al_2O_3$, $Fe_2O_3$ and a small

amount of CaO. The BET specific surface area and water absorption of calcined ash decreased with elevated calcination temperature while the change of density was on the contrary. The content of amorphous phase generated from mineral decomposition increased with calcination temperature. The higher calcination temperature reduced the activity of Al phase resulting in a low dissolution degree of Al. The cooling techniques had negligible effect on physicochemical properties of sludge ash and air cooling was optimal in consideration of energy conservation and environmental protection.

(2) The pozzolanic activity of sludge ash calcined at 800 ℃ and 900 ℃ was confirmed by Frattini test and SAI test. The mortar blended with S8 ash presented the greatest strength activity index as a result of the high content of amorphous phase in ash. The reaction of sludge ash with calcium hydroxide was primarily carried out at early age and the main hydration products were katoite, monocarboaluminate and hemicarboaluminate.

(3) The addition of sludge ash accelerated the formation of ettringite and monosulfate phase resulting in a high initial hydration heat. However, the high Al concentration dissolved from S6 and S7 delayed significantly the cement hydration, especially for $C_3S$, leading to incompetent compressive strength of mortars. Despite the delayed induction period of cement hydration by S8 and S9 ash, the subsequent pozzolanic reaction of sludge ash produced more hydration heat and additional products which filled into the pores and compacted the structure of paste contributing to the strength development of mortars.

(4) The leaching concentrations of heavy metals in mortars blended with sludge ash were far below the regulatory limit. The heavy metals in sewage sludge can be immobilized in ash structure during calcination process and the dense structure of cement paste provided a second barrier for leaching behavior of heavy metals.

# Acknowledgements

The authors gratefully acknowledge financial support from the Key Research and Development Projects of Hunan Province (Grant No. 2020WK2005) and the Postgraduate Scholarship, Central South University, Changsha, China.

# References


[1] A. Raheem, V.S. Sikarwar, J. He, W. Dastyar, D.D. Dionysiou, W. Wang andM. Zhao, Opportunities and challenges in sustainable treatment and resource reuse of sewage sludge: A review, Chem Eng J 337(2018) 616-641.10.1016/j.cej.2017.12.149

[2] G. Yang, G. Zhang andH. Wang, Current state of sludge production, management, treatment and disposal in China, Water Res 78(2015) 60-73.10.1016/j.watres.2015.04.002

[3] M. Praspaliauskas andN. Pedišius, A review of sludge characteristics in Lithuania's wastewater treatment plants and perspectives of its usage in thermal processes, Renewable and Sustainable Energy Reviews 67(2017) 899-907.10.1016/j.rser.2016.09.041

[4] M. Schnell, T. Horst andP. Quicker, Thermal treatment of sewage sludge in Germany: A review, J Environ Manage 263(2020) 110367.10.1016/j.jenvman.2020.110367

[5] A. Kelessidis andA.S. Stasinakis, Comparative study of the methods used for treatment and final disposal of sewage sludge in European countries, Waste Manage 32(2012) 1186-1195.10.1016/j.wasman.2012.01.012

[6] V.D. Katare andM.V. Madurwar, Design and investigation of sustainable pozzolanic material, J Clean Prod 242(2020) 118431.10.1016/j.jclepro.2019.118431

[7] M.C.G. Juenger andR. Siddique, Recent advances in understanding the role of supplementary cementitious materials in concrete, Cement Concrete Res 78(2015) 71-80.10.1016/j.cemconres.2015.03.018

[8] D. Jiapei, B. Yuhuan, C. Xuechao, S. Zhonghou andS. Baojiang, Utilization of alkali-activated slag based composite in deepwater oil well cementing, Constr Build Mater 186(2018) 114-122.https://doi.org/10.1016/j.conbuildmat.2018.07.068

[9] C.J. Lynn, R.K. Dhir, G.S. Ghataora andR.P. West, Sewage sludge ash characteristics and potential for use in concrete, Constr Build Mater 98(2015) 767-779.10.1016/j.conbuildmat.2015.08.122

[10] M. Oliva, F. Vargas andM. Lopez, Designing the incineration process for improving the cementitious performance of sewage sludge ash in Portland and blended cement systems, J Clean Prod 223(2019) 1029-1041.10.1016/j.jclepro.2019.03.147

[11] M. Mejdi, M. Saillio, T. Chaussadent, L. Divet andA. Tagnit-Hamou, Hydration mechanisms of sewage sludge ashes used as cement replacement, Cement Concrete Res 135(2020) 106115.10.1016/j.cemconres.2020.106115

[12] Z. Chen, J.S. Li andC.S. Poon, Combined use of sewage sludge ash and recycled glass cullet for the production of concrete blocks, J Clean Prod 171(2018) 1447-1459.10.1016/j.jclepro.2017.10.140

[13] Z. Chen andC.S. Poon, Comparative studies on the effects of sewage sludge ash and fly ash on cement hydration and properties of cement mortars, Constr Build Mater 154(2017) 791-803.10.1016/j.conbuildmat.2017.08.003

[14] S. Chakraborty, B.W. Jo, J.H. Jo andZ. Baloch, Effectiveness of sewage sludge ash combined with waste pozzolanic minerals in developing sustainable construction material: An alternative approach for waste management, J Clean Prod 153(2017) 253-263.10.1016/j.jclepro.2017.03.059

[15] T. Wang, Y. Xue, M. Zhou, Y. Lv, Y. Chen, S. Wu andH. Hou, Hydration kinetics, freeze-thaw resistance, leaching behavior of blended cement containing co-combustion ash of sewage sludge and rice husk, Constr Build Mater 131(2017) 361-370.10.1016/j.conbuildmat.2016.11.087

[16] W. Piasta andM. Lukawska, The Effect of Sewage Sludge Ash on Properties of Cement Composites, Procedia Engineering 161(2016) 1018-1024.10.1016/j.proeng.2016.08.842

[17] C.J. Lynn, R.K. Dhir, G.S. Ghataora andR.P. West, Sewage sludge ash characteristics and potential for use in concrete, Constr Build Mater 98(2015) 767-779.10.1016/j.conbuildmat.2015.08.122

[18] T.D. Dyer, J.E. Halliday andR.K. Dhir, Hydration Chemistry of Sewage Sludge Ash Used as a Cement Component, J Mater Civil Eng 23(2011) 648-655.10.1061/(ASCE)MT.1943-5533.0000221

[19] M. Cyr, M. Coutand andP. Clastres, Technological and environmental behavior of sewage sludge ash (SSA) in cement-based materials, Cement Concrete Res 37(2007) 1278-1289.10.1016/j.cemconres.2007.04.003

[20] P. Garcés, M. Pérez Carrión, E. García-Alcocel, J. Payá, J. Monzó andM.V. Borrachero, Mechanical and physical properties of cement blended with sewage sludge ash, Waste Manage 28(2008) 2495-2502.10.1016/j.wasman.2008.02.019

[21] M. Coutand, M. Cyr andP. Clastres, Use of sewage sludge ash as mineral admixture in mortars, Proceedings of the Institution of Civil Engineers - Construction Materials 159(2006) 153-162.10.1680/coma.2006.159.4.153

[22] S. Donatello, A. Freeman-Pask, M. Tyrer andC.R. Cheeseman, Effect of milling and acid washing on the pozzolanic activity of incinerator sewage sludge ash, Cement and Concrete Composites 32(2010) 54-61.10.1016/j.cemconcomp.2009.09.002

[23] P. de Azevedo Basto, H. Savastano Junior andA.A. de Melo Neto, Characterization and pozzolanic properties of sewage sludge ashes (SSA) by electrical conductivity, Cement and Concrete Composites 104(2019) 103410.10.1016/j.cemconcomp.2019.103410

[24] Y. Chen, T. Wang, M. Zhou, H. Hou, Y. Xue andH. Wang, Rice husk and sewage sludge co-combustion ash: Leaching behavior analysis and cementitious property, Constr Build Mater 163(2018) 63-72.10.1016/j.conbuildmat.2017.10.112

[25] H. Yanguatin, J.H. Ramírez, A. Tironi andJ.I. Tobón, Effect of thermal treatment on pozzolanic activity of excavated waste clays, Constr Build Mater 211(2019) 814-823.10.1016/j.conbuildmat.2019.03.300

[26] Y. Liu, S. Lei, M. Lin, Y. Li, Z. Ye andY. Fan, Assessment of pozzolanic activity of calcined coal-series kaolin, Appl Clay Sci 143(2017) 159-167.10.1016/j.clay.2017.03.038

[27] A. Tironi, M.A. Trezza, A.N. Scian andE.F. Irassar, Assessment of pozzolanic activity of different calcined clays, Cement and Concrete Composites 37(2013) 319-327.10.1016/j.cemconcomp.2013.01.002

[28] A.R. Pourkhorshidi, M. Najimi, T. Parhizkar, F. Jafarpour andB. Hillemeier, Applicability of the standard specifications of ASTM C618 for evaluation of natural pozzolans, Cement and Concrete Composites 32(2010) 794-800.10.1016/j.cemconcomp.2010.08.007

[29] A. Souri, H. Kazemi-Kamyab, R. Snellings, R. Naghizadeh, F. Golestani-Fard andK. Scrivener, Pozzolanic activity of mechanochemically and thermally activated kaolins in cement, Cement Concrete Res 77(2015) 47-59.10.1016/j.cemconres.2015.04.017

[30] A. Alujas, R. Fernández, R. Quintana, K.L. Scrivener andF. Martirena, Pozzolanic reactivity of low grade kaolinitic clays: Influence of calcination temperature and impact of calcination products on OPC hydration, Appl Clay Sci 108(2015) 94-101.10.1016/j.clay.2015.01.028

[31] S.V. Vassilev, D. Baxter andC.G. Vassileva, An overview of the behaviour of biomass during combustion: Part I. Phase-mineral transformations of organic and inorganic matter, Fuel (Guildford) 112(2013) 391-449.10.1016/j.fuel.2013.05.043

[32] L. Kovarik, M. Bowden andJ. Szanyi, High temperature transition aluminas in δ-Al2O3/θ-Al2O3 stability range: Review, J Catal 393(2021) 357-368.10.1016/j.jcat.2020.10.009

[33] L. Nicoleau, E. Schreiner andA. Nonat, Ion-specific effects influencing the dissolution of tricalcium silicate, Cement Concrete Res 59(2014) 118-138.10.1016/j.cemconres.2014.02.006

[34] A. Schöler, B. Lothenbach, F. Winnefeld, M.B. Haha, M. Zajac andH. Ludwig, Early hydration of SCM-blended Portland cements: A pore solution and isothermal calorimetry study, Cement Concrete Res 93(2017) 71-82.10.1016/j.cemconres.2016.11.013

[35] P. Bénard, S. Garrault, A. Nonat andC. Cau-Dit-Coumes, Hydration process and rheological properties of cement pastes modified by orthophosphate addition, J Eur Ceram Soc 25(2005) 1877-1883.10.1016/j.jeurceramsoc.2004.06.017

[36] M. Mejdi, M. Saillio, T. Chaussadent, L. Divet andA. Tagnit-Hamou, Hydration mechanisms of sewage sludge ashes used as cement replacement, Cement Concrete Res 135(2020) 106115.10.1016/j.cemconres.2020.106115

[37] T. Matschei, B. Lothenbach andF.P. Glasser, The AFm phase in Portland cement, Cement Concrete Res 37(2007) 118-130.10.1016/j.cemconres.2006.10.010

[38] J. Kaufmann, R. Loser andA. Leemann, Analysis of cement-bonded materials by multi-cycle mercury intrusion and nitrogen sorption, J Colloid Interface Sci 336(2009) 730-737.10.1016/j.jcis.2009.05.029

[39] N. De Belie, J. Kratky andS. Van Vlierberghe, Influence of pozzolans and slag on the microstructure of partially carbonated cement paste by means of water vapour and nitrogen sorption experiments and BET calculations, Cement Concrete Res 40(2010) 1723-1733.10.1016/j.cemconres.2010.08.014

[40] C.J. Lynn, R.K. Dhir andG.S. Ghataora, Environmental impacts of sewage sludge ash in construction: Leaching assessment, Resources, Conservation and Recycling 136(2018) 306-314.10.1016/j.resconrec.2018.04.029

[41] X.D. Li, C.S. Poon, H. Sun, I.M. Lo andD.W. Kirk, Heavy metal speciation and leaching behaviors in cement based solidified/stabilized waste materials, J Hazard Mater 82(2001) 215-230.10.1016/s0304-3894(00)00360-5

[42] D. de Almeida Lima andC. Zulanas, Use of Contaminated Sludge in Concrete, Procedia Engineering 145(2016) 1201-1208.10.1016/j.proeng.2016.04.155

[43] B. Guo, B. Liu, J. Yang andS. Zhang, The mechanisms of heavy metal immobilization by cementitious material treatments and thermal treatments: A review, J Environ Manage 193(2017) 410-422.10.1016/j.jenvman.2017.02.026

[44] R. Li, W. Zhao, Y. Li, W. Wang andX. Zhu, Heavy metal removal and speciation transformation through the calcination treatment of phosphorus-enriched sewage sludge ash, J Hazard Mater 283(2015) 423-431.10.1016/j.jhazmat.2014.09.052

[45] Q.Y. Chen, M. Tyrer, C.D. Hills, X.M. Yang andP. Carey, Immobilisation of heavy metal in cement-based solidification/stabilisation: A review, Waste Manage 29(2009) 390-403.10.1016/j.wasman.2008.01.019

## Highlights

- Physicochemical properties and pozzolanic activity of sludge ashes were investigated.
- The sludge ash calcined at 800℃ presented high pozzolanic activity.
- Sludge ash addition enhanced the formation of Al-bearing hydrates.
- No leaching risk was detected for the use of sludge ash in building material.